

University of Montana

ScholarWorks at University of Montana

Graduate Student Theses, Dissertations, &
Professional Papers

Graduate School

1996

Continental Phenology Modeling

Michael White

The University of Montana

Follow this and additional works at: <https://scholarworks.umt.edu/etd>

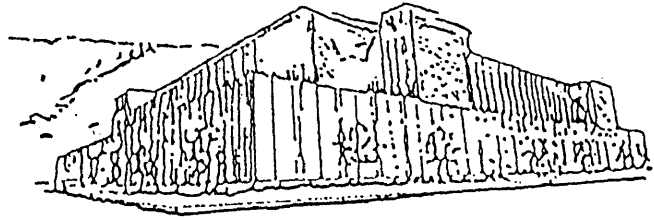
Let us know how access to this document benefits you.

Recommended Citation

White, Michael, "Continental Phenology Modeling" (1996). *Graduate Student Theses, Dissertations, & Professional Papers*. 5661.

<https://scholarworks.umt.edu/etd/5661>

This Thesis is brought to you for free and open access by the Graduate School at ScholarWorks at University of Montana. It has been accepted for inclusion in Graduate Student Theses, Dissertations, & Professional Papers by an authorized administrator of ScholarWorks at University of Montana. For more information, please contact scholarworks@mso.umt.edu.



Maureen and Mike
MANSFIELD LIBRARY

The University of **MONTANA**

Permission is granted by the author to reproduce this material in its entirety,
provided that this material is used for scholarly purposes and is properly cited in
published works and reports.

*** Please check "Yes" or "No" and provide signature ***

Yes, I grant permission
No, I do not grant permission

Author's Signature Michael White

Date 6/12/96

Any copying for commercial purposes or financial gain may be undertaken only with
the author's explicit consent.

CONTINENTAL PHENOLOGY MODELING:

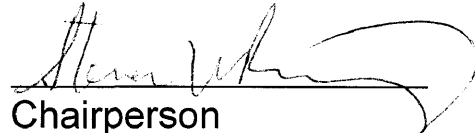
by

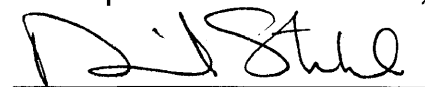
Michael White

B.A. The University of Virginia

presented in partial fulfillment of the requirements
for the degree of
Master of Science
The University of Montana
1996

Approved by:


Chairperson


Dean, Graduate School

7-19-96
Date

UMI Number: EP41125

All rights reserved

INFORMATION TO ALL USERS

The quality of this reproduction is dependent upon the quality of the copy submitted.

In the unlikely event that the author did not send a complete manuscript and there are missing pages, these will be noted. Also, if material had to be removed, a note will indicate the deletion.



UMI EP41125

Published by ProQuest LLC (2014). Copyright in the Dissertation held by the Author.


Microform Edition © ProQuest LLC.

All rights reserved. This work is protected against unauthorized copying under Title 17, United States Code



ProQuest LLC.
789 East Eisenhower Parkway
P.O. Box 1346
Ann Arbor, MI 48106 - 1346

Continental Phenology Modeling

Director: Steven W. Running 

Regional phenology is an important variable in ecosystem simulation models and coupled biosphere/atmosphere models. In the continental U.S., the timing of the onset of greenness in the spring (leaf expansion, grass green-up) and offset of greenness in the fall (leaf abscission, cessation of height growth, grass brown-off) are strongly influenced by meteorological and climatological variables. My objective was to develop phenology models to predict the timing of onset and offset at a regional ecosystem level and to scale them to a continental level. I developed predictive models based on traditional phenology research using only commonly available meteorological and climatological data, and obtained phenology observations from satellite methodologies. Onset mean absolute errors are 7.6 days in the tree biome with an r^2 of 0.76 and 5.9 days in the grass biome with an r^2 of 0.85. Offset mean absolute errors are 5.5 days in the tree biome with an r^2 of 0.44 and 7.5 days in the grass biome with an r^2 of 0.89. Onset is strongly associated with temperature summations in both grass and tree biomes; tree offset is best predicted with a photoperiod function while grass offset requires a combination of precipitation and temperature controls. I was unable to develop accurate models for crop and desert and desert biomes. Continental application of the phenology models for 1990-1992 reveals extensive interannual variability in onset and offset. Mean continental growing season length ranged from a low of 140 days in 1990 to a high of 154 days in 1992.

Acknowledgments

After spending my first two years out of college in a kitchen, it was quite a shock to sit down at my desk and ask “UNIX, what’s UNIX?” or, “what do you mean, I have to compile the program?” For their patient assistance with these and all other inquiries, I am grateful to Peter Thornton and Joseph White. I also thank Steve Running for bringing me into the lab and for providing inspiration, encouragement, and the freedom to pursue all my inquiries. Thanks to Ramakrishna Nemani for insightful suggestions, numerous remote sensing discussions, and all that spinach. I greatly appreciate the support, advice, and helpful comments I received from committee members Roly Redmond and Lloyd Queen. Thank you to the rest of NTSG: Deb Kendall, Jodi Gibbons, Saxon Holbrook, Galina Churkina, John Kimball, Kathy Hibbard, and Joe Glassy. Joy Hood at EROS and Nan Rosenbloom at NCAR provided critical datasets, and for that I am especially grateful. Thanks and love to Stephanie Best for coming to Missoula, having faith, and everything else.

Table of Contents	page
Title page	
Abstract	ii
Acknowledgments	iii
Table of Contents	iv
List of Tables	v
List of Figures	vi
Introduction and Background	1
Methods	6
Satellite Observations	6
Satellite Detection of Onset and Offset	9
Ground Observations	10
Meteorological Interpolation	11
Model Development	15
Results	17
MT-CLIM 3d	17
BISE and Detection of Onset and Offset	18
Model Building	19
Discussion	26
Summary and Results	32
References	34
Tables	42
Figures	45

List of Tables

Table 1 (page 42).
Satellite phenology detection methodologies

Table 2 (page 43).
Hubbard Brook Experimental Forest phenology measurement scheme

Table 3 (page 44).
MT-CLIM 3d cross validation results

List of Figures

Figure 1 (page 45).

Best Index Slope Extraction from raw AVHRR data. Points represent AVHRR observations from one pixel for one year. Solid line is the fitted curve. The NDVI curve from (a) is transformed into a ratio from 0-1 in (b). Onset is predicted at the yearday when $NDVI_{ratio}$ exceeds 0.5; offset is predicted when $NDVI_{ratio}$ falls below 0.5. Striped area is the green period; shaded area is non-green period.

Figure 2 (page 46).

Weather station distribution.

Figure 3 (page 47).

Satellite Phenology Observation Sites. Distribution of 20km x 20km study sites. Daily AVHRR observations were archived at each site for 1990-1992.

Figure 4 (page 48).

Three-year mean and difference from mean MT-CLIM 3d results. Large panels represent average conditions from 1990-1992. Small panels illustrate variation between years.

Figure 5 (page 49).

Comparison of field observations and satellite observations. The curves represent trends of field-measured leaf. Squares are superimposed on the curve at the day of satellite-observed onset or offset. For example, in fig. 5a, onset was observed on yearday 140 in 1990, yearday 125 in 1991, and yearday 139 in 1992. Average leaf expansion at satellite-observed onset is calculated as 30%.

Figure 6 (page 50).

TAVG (1990-1992) vs. Soil Temp Summation at Onset. At each site, the three-year mean air temperature is plotted on the x-axis. The three-year mean thermal summation extracted from the meteorological files at the date of satellite-observed onset is plotted on the y-axis. An exponential function was fitted to the tree points (a) and an asymptotic function to the grass points (b).

Figure 7 (page 51).

Predicted versus observed results in grass and tree biomes.

Figure 8 (page 52).

Ecosystem phenology applied to continental scales. Upper panels illustrate onset; lower panels illustrate offset. Middle panels are frequency distributions of growing season length.

Introduction and Background

Vegetation phenology, the study of recurring vegetation cycles and their connection to climate, is an important variable in a wide variety of earth and atmospheric science applications. In particular, as interest in global change research grows, accurate phenology models will become increasingly vital tools, enabling researchers to investigate the impacts of climatic variability on vegetation dynamics in the past and future. The presence or absence of a photosynthetically active canopy has dramatic effects on regional to global ecosystem simulation models (Running and Nemani, 1991; Goetz and Prince, 1996), coupled biosphere/atmosphere General Circulation Models (GCM's) (Sellers et al., 1996), and land surface parameterization schemes (Henderson-Sellers et al., 1993). In these applications, the timing and the length of the growing season controls the spatiotemporal dynamics of crucial carbon and water cycles and strongly influences latent/sensible heat transport (Schwartz, 1992).

Phenology is highly variable (Scmidt and Lotan, 1980) and tied to long-term variation in climate (Sparks and Carey, 1995). The goal of my research was to develop a simple model capable of representing this climatically-induced phenological variability at a regional level in the continental U.S.. Central features of the methodology include biome-specific models and simple data requirements consisting only of

commonly available meteorological and climatological variables. A major difficulty presented by this goal is a fundamental scale discontinuity. GCM's and ecosystem simulation models are incapable of capturing species level detail, but most phenological research has focused on single species or geographic areas. In spite of this narrow focus, several consistent literature findings indicate starting points from which to construct regional models.

In trees, the initiation of the growing season, or onset of greenness, has been successfully modeled using a cumulative thermal summation (degree-days). The technique dates to Reamur (1735) and is extremely simple. After an arbitrary start date (usually January 1) mean air temperature or soil temperature over an arbitrary threshold (usually 0°C or 5°C) is summed until a critical value is exceeded, at which point the proscribed phenological event is predicted to occur (Hickin and Vittum, 1976; Thomson and Moncrieff, 1981; Cannel and Smith, 1986; Murray et al., 1989; Harri and Häkkinen, 1991; Hunter and Lechowicz, 1992; Caprio, 1993; Hänninen et al., 1993). Most trees must fulfill a chilling requirement before warmer temperatures begin to affect springtime growth, and some models include this parameter (Lavender, 1981). Lindsay and Newman (1956) and Valentine (1983), however, successfully ignored chilling requirements.

Extensive literature reviews strongly suggest that short days induce dormancy, or offset of greenness, (cessation of height growth, development of cold hardiness, abscission) in woody plants (Vegis, 1964; Nooden and Weber,

1978). It appears that the critical daylength varies with latitude such that northern populations become dormant with relatively long days while southern populations continue growth to much shorter days (Heide, 1974; Hänninen et al., 1990; Oleksyn et al., 1992). Further, the growing season can be prolonged by warm temperature and curtailed by cold temperatures (Heide, 1974; Smit-Spinks et al., 1985; Koski and Selkäinaho, 1982).

In other biomes, growth is influenced by a variety of factors. Grasslands are sensitive to temperature, precipitation (French and Sauer, 1974; Mueggler, 1983), and soil moisture (Dickinson and Dodd, 1975). Growth in dry grasslands is controlled largely by moisture (Kemp, 1983) while grasslands in cooler, moister areas are limited primarily by temperature (Ram et al., 1988). Grassland ecosystems will remain green until the growing season is curtailed by heat, drought, or cold (). Growth in desert shrub/grasslands is largely controlled by precipitation and drought stresses (Sharifi et al., 1988; Kemp, 1983; Burk, 1982). Crop phenology is uniquely independent of an immediate tie to natural phenological influences. Knowledge of factors such as genotype, planting time, fertilization, irrigation, and harvest time can lead to accurate phenological models for specific crops (Doraiswamy and Thompson, 1982; Lomas and Herrera, 1985; O'Leary et al., 1985; Brown, 1986; Hodges and French, 1985; Undersander and Christiansen, 1986); purely meteorological or climatological influences are inadequate inputs.

Since many models are driven by meteorological information, either from actual daily records or stochastically generated daily records from monthly means, meteorology is a viable driver for phenology models. But to develop and test models, observations of phenology are required. At the large scales in question, it is extremely difficult to obtain consistent field phenology observations across landcovers which represent general ecosystem activity, rather than the phenology of one or two species. To overcome this difficulty, numerous studies have used daily coverage of the terrestrial biosphere by the National Oceanic and Atmospheric Administration (NOAA) Advanced Very High Resolution Radiometer (AVHRR) to quantify ecosystem vegetation phenology. The normalized difference vegetation index (NDVI), calculated as $(N-R) / (N+R)$, where N is the near infrared reflectance and R is the red reflectance, has been related to several biophysical parameters including chlorophyll density (Tucker et al., 1985), percent canopy cover (Yoder and Waring 1994), absorbed photosynthetically active radiation (Myneni and Williams, 1994), leaf area index (Spanner et al., 1990b), and productivity (Prince et al., 1995). Potentially, NDVI ranges from -1 to 1, but earth surfaces are usually limited to -0.1 to 0.7 NDVI.

Early in the history of satellite phenology research, Justice et al. (1985) used the NDVI to qualitatively assess the global phenology of numerous landcover types. Goward et al. (1985) demonstrated that the NDVI corresponds to known seasonality in the continental U.S.. Satellites were later used to interpret phenology as an indicator of landcover changes in South America

(Stone et al., 1994) and detect phenological dynamics in shrublands (Duncan et al., 1993). A variety of methods have been used to attach quantitative dates of onset and offset to satellite data (Table 1). Clearly, there are numerous quantitative methodologies in use, each somewhat arbitrary and unique to a specific question.

In this paper, I integrate the basic concepts of traditional meteorologically-based phenology modeling with intensive satellite phenology observations to produce biome-specific ecosystem phenology models. This research is intended as a complement and alternative to satellite estimates of seasonal dynamics. For current and relatively recent modeling efforts, global seasonality can be established from satellite data. Meteorology-driven phenology models will be useful in situations where a time series of satellite imagery is not available. Obvious examples include: research based on high spatial / low temporal resolution satellites (Thematic Mapper); historical research for which only meteorology is available; and testing impacts of climate change scenarios on vegetation dynamics (VEMAP, 1995) . For these situations and situations in which the user does not wish to expend the resources required to generate satellite phenology estimates, a meteorological model is crucial.

Methodology

Satellite Observations

I obtained a United States Geological Survey (USGS) Earth Resource Observation Systems (EROS) dataset of daily NOAA-11 AVHRR observations for 56 20km x 20km study sites within the continental U.S. and southern Canada (Hood, 1993). The sites were selected at areas of general scientific interest and contiguous landcover. From 1990 - 1992, the five AVHRR channels, satellite zenith angle, solar zenith angle, relative azimuth angle, date, and time of acquisition were recorded for all sites. Due to difficulties in geometric registration, satellite overpasses with extensive cloud cover were not archived. Consequently, at a given site, it is possible to have two overpasses on the same day, or to have no observations for several days. If two overpasses occurred on the same day, I selected the higher NDVI value. Archived data were corrected by EROS for sensor degradation using radiometric calibrations based on preflight gain coefficients and for solar illumination variability using the cosine of the zenith angle (Hood, 1993). Images were registered to a Lambert's Azimuthal Equal Area projection. Based on findings by Goward et al. (1991) suggesting that extremely off-nadir view angles result in exponentially increasing footprints and severe reflectance and anisotropy difficulties, I screened the data to remove observations greater than $> 50^\circ$ off-nadir, resulting in approximately a 25% reduction in usable NDVI data.

Studies of vegetation dynamics usually process AVHRR daily images using a maximum value compositing technique (Holben, 1986). Within a compositing period, usually two weeks but often longer in chronically cloud-covered areas, the maximum NDVI is selected on a pixel by pixel basis, resulting in a complete, hopefully cloud-free image pieced together from multiple overpasses. A further screening process is often added to eliminate observations with extremely off-nadir satellite view angles. The main assumption of the maximum value compositing technique is that non-optimal atmospheric, soil, view and illumination angle conditions depress the NDVI and that the maximum NDVI in the composite period best represents actual vegetation status. Despite the considerable advantages of this methodology (reduction in cloud contamination and data volume), there is an inevitable loss of temporal resolution.

Since maintaining the temporal detail of the original dataset was a priority, I used an alternate processing technique. The Best Index Slope Extraction (BISE) provides a methodology which preserves the unique temporal resolution of the dataset while reducing the effects of cloud contamination, atmospheric interference, and bidirectional reflectance (Viovy and Arino, 1992). The BISE algorithm contains three assumptions: 1) NDVI is depressed by cloud and atmospheric contamination; 2) data transmission errors, such as line drop, will result in short, abnormally high deviations from the general NDVI trend; 3) rapid,

non-persistent increases or decreases in NDVI are inconsistent with natural vegetation growth.

Fig. 1a demonstrates an application of the BISE algorithm to one year of raw AVHRR observations for one pixel. An ascending curve is fitted to any high points which do not exceed a truncation threshold and a descending curve is fitted to any points which are not isolated, large decreases in NDVI. The algorithm searches forward from the first date and selects the next point if it is higher. Point to point increases in NDVI greater than the truncation threshold are ignored. If there is a decrease in NDVI from one value to the next, it is accepted only if there is no point within a user defined sliding period which is greater than 20% of the difference between the previous high and current low point. If such a value does occur, it is selected and the low point is ignored. Note that rapid decreases in NDVI will be accepted provided they are persistent. Once BISE has selected the data points for a given time series, a curve is fit to the time series using a linear extrapolation.

BISE is sensitive to the length of the sliding period and to the magnitude of the truncation threshold. Too long a sliding period may miss natural vegetation changes while too short a sliding period will result in extremely noisy NDVI curves; truncation thresholds must allow for rapid growth while rejecting abnormally large jumps. Viovy and Arino (1992) found that 1) a 30 day sliding period works best but that a 40 day sliding period produced no apparent adverse

consequences and 2) a truncation threshold of 0.1 removed aberrant NDVI jumps unrelated to normal vegetation activity.

Since the goal of this research is to analyze regional phenological trends, not to investigate within site phenological variability or spatial autocorrelation, I ran BISE for each of the 400 pixels at all 56 sites and averaged the curves, producing one NDVI curve for each site. I assume that the single output NDVI curve represents the general trend of ecosystem greenness at each site.

Satellite Detection of Onset and Cessation

The state of the ecosystem (green, non-green) is assessed using a ratio of the NDVI:

$$(1) \quad NDVI_{ratio} = \frac{NDVI - NDVI_{min}}{NDVI_{max} - NDVI_{min}}$$

where $NDVI_{ratio}$ is the output ratio, ranging from 0 - 1, $NDVI$ is the daily NDVI, $NDVI_{max}$ is the annual maximum NDVI, and $NDVI_{min}$ is the annual minimum NDVI.

An $NDVI_{ratio}$ of 0 represents the annual minimum NDVI while an $NDVI_{ratio}$ of 1 represents the annual maximum NDVI. This methodology is attractive primarily because of its consistency across vegetation type. An $NDVI_{ratio}$ of 0.5 implies that a site has attained half its maximum NDVI regardless of the absolute NDVI

magnitude. Consequently, a single $NDVI_{ratio}$ threshold may be used, obviating the need to establish absolute NDVI thresholds or landcover-specific thresholds. The onset of greenness is predicted to occur on the yearday at which $NDVI_{ratio}$ of 0.5 is exceeded; offset is predicted when $NDVI_{ratio}$ falls below 0.5 (Fig. 1b). Using this methodology, I predicted dates of onset and offset of greenness for the 56 site for 1990 - 1992.

Ground Observations

Researchers at two satellite study sites (Harvard Forest and Hubbard Brook Experimental Forest Long Term Ecological Research (LTER) sites) collected detailed phenological measurements for 1990 - 1992. At the Harvard Forest, dates of development at initial budburst, 75% of total leaf expansion, greater than 95% of total leaf expansion, onset of fall color, 10%-25% leaf fall, and 95% leaf fall were recorded for 33 understory and overstory species at 3-7 day intervals from April through June. Using a representative sample of dominant overstory and understory tree species (O'Keefe, personal communication), I compiled average dates for each developmental stage. At Hubbard Brook, data were recorded in the spring and fall for American beech (*Fagus grandifolia*), sugar maple (*Acer saccharum*), and yellow birch (*Betula alleghaniensis*) at eight plots. Three dominant or codominant individuals of each species were marked and sampled at each plot using the numerical scheme presented in Table 2. I compiled average development dates for each species at each plot and

averaged all eight plots. I determined if the dates of onset and offset of greenness extracted from the satellite methodology corresponded to field observations, and if so, to what developmental stage.

Meteorological Interpolation

PREPROCESSOR STEPS: I used MTCLIM-3d, a methodology developed by Thornton et al. (in press), to generate daily surfaces of temperature, precipitation, and radiation over the continental U.S. As inputs, MTCLIM-3d requires daily weather station observations, station locations and elevations, and a digital elevation model (DEM). Daily outputs include maximum and minimum temperature in °C (TMAX and TMIN), precipitation in cm (PPT), daylength in minutes (DAYL), and short wave radiation in average daylight watts m⁻² (RAD).

I obtained 1168 daily TMAX, TMIN, and PPT records within the continental U.S. from the National Center for Atmospheric Research (Fig. 2). Station distribution, correlated with population density, is high throughout much of the eastern U.S., the Puget Sound area, and the Wasatch Front in central Utah. Station density is low in sparsely populated, desert areas such as southern Nevada, Maine, and Death Valley, California. I discarded station records which contained more than 25 missing days in one year or more than five consecutive missing days. For remaining records which still contained missing days, I used a linear interpolation to fill missing temperature data, set missing precipitation values to 0.0 cm, and set trace precipitation to 0.01 cm.

In order to keep file sizes and computational time at a manageable level while retaining a relatively fine level of topographic detail, I generated output surfaces at a 10km resolution. Pixels are defined by a 1km DEM resampled to a 10km resolution. Elevations are averaged; nearest neighbor resampling results in spatially discontinuous elevations. Station locations, recorded only to the nearest arc minute, contain a possible location range of several kilometers. Station elevations, recorded to the nearest meter, are considered to be more accurate. I corrected recorded station elevations and locations by assigning station locations to the pixel in a 30km x 30km search area around the recorded location which minimized the error between the recorded and DEM elevation.

INTERPOLATION: A truncated gaussian filter is the central tool of the interpolation methodology. Interpolations are calculated from weather station observations where the station location on the filter determines the observation weight. Truncation, by removing large numbers of stations with low weights, dramatically increases computational speed with only a small loss of surface smoothness. Weighting of the gaussian filter from the central point, p , is calculated as:

$$(2) \quad W_r = e^{\left(\frac{r}{R_p}\right)^\alpha} - e^{-\alpha}$$

where W_r is the filter weight at radial distance, r , from p , R_p is the truncation distance from p , and α is a dimensionless shape parameter. R_p is spatially varied in an iterative process such that an average number of stations, N , is achieved over the study area. From an initial estimate, R_p is adjusted upward or downward based on the local station density. Thus, R_p is smaller in high density areas and larger in low density areas. For each grid cell, a list of stations and weights within R_p is calculated.

Temperature predictions, T_p , are calculated as:

$$(3) \quad T_p = \frac{\sum_{i=1}^n W_i (T_i + E_i)}{\sum_{i=1}^n W_i}$$

where n is the number of observations, W_i is the observation weight, T_i is the temperature observation, and E_i is a daily elevation-based correction to temperature calculated from a weighted least squares regression equation.

Precipitation predictions, P_p , are calculated only if a precipitation event is first predicted. Essentially, if the precipitation occurrence probability, POP , calculated from weighted precipitation occurrences within the filter radius, is greater than a critical value, POP_{crit} , a precipitation event is generated. If so, precipitation is calculated as:

$$(4) \quad P_p = \frac{\sum_{i=1}^n W_i PO_i \left(\frac{1 + E_p}{1 - E_p} \right)}{\sum_{i=1}^n W_i PO_i}$$

where PO_i is a binomial variable (1=precipitation, 0=no precipitation) and E_p is a daily elevation-based correction to precipitation calculated from a weighted least squares regression. Prediction weights, then, are assigned only to those observations at which precipitation is recorded. Additionally, if E_p is greater than E_{pmax} , E_p is set to E_{pmax} . Inclusion of E_{pmax} is necessary because regression equations calculated from low elevation observations and extrapolated to high elevations can result in extremely large predictions if a truncation is not introduced.

Incident short wave radiation is calculated using daylength, earth-sun geometry, assumptions regarding atmospheric transmissivity, optical air mass,

and diurnal temperature range. For a detailed description of radiation and daylength calculations, see Thornton, et al. (in press), Hungerford et al. (1989), Bristow and Campbell (1984), Glassy and Running (1994), Running et al. (1987).

Diffuse and direct radiation are calculated at a minute timestep, summed, and divided by daylength, producing daylight radiative flux density in W m^{-2} .

I used a cross-validation analysis to assess the effects of varying input parameters. Using initial parameter estimates, station observations are withheld and predicted from remaining observations. The predicted value can then be compared to the withheld, observed value, and the difference quantified. In an iterative process, the combination of parameters is varied until the daily and annual mean absolute error (MAE) and bias of the predicted versus observed TMAX, TMIN, and PPT are minimized. The optimized parameters are then applied to the entire interpolation.

Model Development

I combined three tools to develop the phenological models: 1) satellite observations of onset and offset, 2) landcover at each site, and 3) climatological and meteorological data. The basic methodology was to subdivide study sites into landcover groupings and to determine, based on traditional phenological functions, what combination of meteorological equations will best predict the satellite-observed dates of onset and offset for each landcover group. Hood (1993) provided a highly detailed landcover classification based on Loveland

(1991). However, in the interests of generality and repeatability, I used a satellite-based landcover map developed by Nemani and Running (1995) consisting of six landcover classes: 1) barren/sparse vegetation, 2) evergreen shrub, 3) grass (including cereal crops), 4) broadleaf crops, 5) evergreen needleleaf forest, and 6) deciduous broadleaf forest. I grouped classifications by Hood (1993) into one of Nemani and Running's six classes (Fig. 3) and further grouped classes 5 and 6 into a tree class. Sites classified by Hood (1993) as Canadian, urban, barren, and wetland sites were removed from the analysis.

For each biome, I analyzed onset and offset with a suite of climatological and meteorological variables. I followed a basic two step methodology: 1) use the satellite-observed dates of onset and offset as pointers to dates in the meteorological files and 2) identify the general meteorological or climatological conditions at those dates which would best predict the satellite-observed dates. Within the forest classes (class 5 and 6), I focused primarily on soil temperature summations to predict onset (soil temperature calculated as an 11-day running average after Zheng, 1993) and photoperiod to predict offset. Barren/sparse vegetation (class 1) was not modeled due to its lack of vegetation dynamics. Assuming that evergreen shrub (class 2), grass (class 3), and crop (class 4) were dominated by precipitation and temperature controls, I applied a variety of precipitation stress indicators, absolute temperature limitations, and temperature summations. Once initial phenology models were developed and executed, I compared the predicted dates of onset and offset with the satellite observations

and began a process of refining the models to reduce the MAE associated with the predictions. Following final model development, I completed continental runs in which the landcover image was integrated with the model equations to produce images of onset and offset for the continental U.S.

Results

MTCLIM-3d

Final cross-validation results for MTCLIM-3d are presented in Table 3. Daily temperature MAE ranges from 1.76 °C to 1.93 °C with TMIN MAE consistently lower than TMAX MAE. At an annual scale the pattern is reversed, where TMIN MAE consistently exceeds TMAX MAE, with values ranging from 0.77 °C to 1.00 °C. Bias is consistently low for TMAX and TMIN. As a percent, annual and daily errors for PPT are highest for 1990, with an MAE of 21.8% and a bias of 9.9%. Measured in cm, though, 1991 has the highest errors, with an MAE of 13.0 cm and a bias of -0.66 cm. In general, error statistics are similar to errors found by Thornton et al. (in press).

Figure 4 illustrates spatial and temporal variability in temperature and precipitation. The upper large image shows that in the East, temperature increases from north to south while in the West, the influence of the Rocky Mountains, large riparian zones, basin and range topography, and the presence of large deserts create a more varied pattern. The difference from mean panels illustrate that 1990 was generally hot and that 1992, the year after the Mt.

Pinatubo eruption, was cool, especially in the East. Mean PPT is sharply divided between wet and dry areas by a north-south border running approximately along the short/tall grass prairie division. To the east of the border, PPT is highest in the south; to the west of the border, PPT, strongly influenced by topography, is more variable. Difference from mean images underscore this pattern, showing that in each of the three study years, high PPT areas were located in different western regions. In the east, the location of the Texas to New England storm track shifted in each year: north in 1990, south in 1991, and even further south in 1992.

BISE and detection of onset and offset

Initial BISE runs with the default 30 day sliding period revealed that in some cases, the off-nadir screening had removed a quantity of values sufficient to cause numerous failures in the curve fitting algorithm. The problem occurs if there are no observations within the length of the sliding period, in which case 30 consecutive days are set to 0. Increasing the sliding period to 40 days removed this problem without detracting from the algorithm's ability to detect rapid decreases in NDVI. The default truncation threshold of 0.1 NDVI removed artificially large jumps in NDVI while still allowing for periods of sharply increasing growth.

Fig. 5 suggests that satellite-based estimates of onset and offset are comparable to the same general states of phenological development at the

Harvard Forest and Hubbard Brook LTER sites. At the Harvard Forest, the satellite observations of onset correspond to an average of 30% leaf expansion in the spring (Fig. 5a) while observations of offset correspond to an average of 15% leaf drop in the fall (Fig. 5b). At Hubbard Brook, observed onset occurred at an average stage of 1.8, which represents leaves in the initial stages of expansion, or about 1cm long (Fig. 5c). Offset occurred at an average value of 1.6, or roughly 30% leaf fall (Fig. 5d). Although considerable variability exists, especially at Hubbard Brook, and offset data was unavailable at the Harvard Forest for 1990, results suggest that an $NDVI_{ratio}$ of 0.5 corresponds to a ground state of initial leaf expansion (1 cm or 30%) in the spring and to a 15% to 25% leaf drop in the fall.

Model Building

TREE: Initially, I believed that one degree day summation or precipitation level could be found to represent onset. Within the deciduous broadleaf forest landcover type (sites 10, 12-15, and 17-19), for example, it seemed plausible that all sites might require the same degree of warming to initiate growth. This did not prove to be the case. The range of thermal summations varied from a low of 103 °C to a high of 813 °C. Using one thermal summation resulted in poor predictions. If the climate of the site is taken into consideration, though, results were vastly improved. Figure 6a demonstrates that the average thermal

summation required to initiate onset is an exponential function of the 1990-1992 mean annual temperature, where the equation for the line is:

$$(5) \quad STSUM_{crit} = e^{(4.99695+0.109667TAVG)}$$

Where TAVG is the 1990-1992 mean air temperature. Essentially, to induce onset, warmer sites require a larger thermal summation than cool sites. Using this equation alone, MAE is 7.5 days. The addition of a radiation summation, calculated as one standard deviation below the mean radiation summation at onset, reduced MAE to 6.8 days. Addition of precipitation parameters did not affect the MAE. Onset is predicted to occur when:

$$(6) \quad \sum_0^i STSUM \geq STSUM_{crit} \ \& \ \sum_0^i RADSUM \geq RADSUM_{crit}$$

where $STSUM$ is a soil temperature summation with a threshold of 0° , $STSUM_{crit}$ is the summation critical value, $RADSUM$ is a radiation summation, and $RADSUM_{crit}$ is the radiation summation critical value. I calculated summations and critical values using air temperatures and soil temperatures; results were similar in all cases, but using mean air temperature for the critical value and soil temperature for the summations produced marginally superior results.

Since broadest possible applicability was a primary consideration, I experimented with adding other landcover types to the basic deciduous predictions. Using the model developed for the deciduous sites, I generated predictions for coniferous sites (1,4, and 6) and recalculated errors for the combined classes. MAE increased slightly to 7.3 days. Addition of the mixed

forest/cropland site (11) increased MAE to 7.6 days. Addition of sites classified as crop/woodland (sites 24, 37, and 38) dramatically increased MAE. Effectively, then, all tree sites can be grouped together with an onset prediction accuracy of about one week and an r^2 of 0.76 (Fig. 7a).

Photoperiod alone could be used to reasonably predicted offset. The photoperiod associated with satellite observed offset was nearly constant across all tree sites, with a mean value of 648 minutes. Using this trigger value alone, MAE was 6.5 days. Since much research has suggested that photoperiod triggers are active only within a certain temperature range, I added upper and lower limits. If the temperature is warm, growth is permitted to continue while extremely low temperatures will induce offset regardless of photoperiod. I empirically determined the upper soil temperature range to be 12°C and the lower range to be 2°C, reducing MAE to 6.2 days. Slightly increasing the critical daylength to 655 minutes lowered MAE to 5.5 days, with an r^2 of 0.42 (Fig. 7b).

GRASS: Onset of greenness in the grassland sites was strongly controlled by temperature. A relationship of average annual air temperature and predicted summation indicated that a strongly exponential function could predict appropriate summations. However, for high temperature grasslands, such as in Texas, this equation predicted summations which were never reached. The lower temperature sites (2,3,5, and 7), clustered around 7°C mean annual temperature, all required a summation of about 400°C, while the warmer site in Nebraska (site 8) required a summation of 1250°C. Additionally, the cool sites

were also considerably drier than the Nebraska site, suggesting that different grass types may require different summations. In order to maintain one equation for the entire landcover type while still allowing for a division for between vegetation types, I implemented a strongly asymptotic function of the form:

$$(7) \quad GRASS_{stsum} = \left(\frac{1000}{1 + 2000e^{(-2.25TAVG+14)}} \right) + 400$$

The lower limit of predicted thresholds is 400°C, as proscribed by the cool temperature sites. The curve becomes asymptotic near an average annual air temperature of 13°C and remains constant above 15°C (Fig. 6b), defined by Sims (1988) as the upper temperature limit to most grasslands. Using this equation, onset was predicted with a MAE of 6.2 days.

For model building in the study sites, addition of precipitation parameters did not improve results. Nonetheless, in dry grasslands areas (not available in satellite database), sufficient moisture is a required precursor to growth. To account for this necessity in the model, I included a precipitation summation requirement of the form:

$$(8) \quad \text{Grass}_{\text{pptsuncrit}} = k \text{PPT}_{\text{avg}}$$

where k is a % of the average annual precipitation for the site. I increased k to 15% at which point MAE began to increase. Thus, grassland must attain sufficient moisture (Eq. 8) and temperature summations (Eq. 7) before onset is predicted to occur. Again seeking greater applicability, I experimented with including other landcover classes and found that addition of the woodland/pasture class (sites 9 and 16) slightly reduced onset MAE to 5.9 days. Inclusion of mixed crop sites, as in the tree biome, significantly degraded results. Figure 7c demonstrates that grassland onset was predicted with an accuracy of less than one week and an r^2 of 0.85.

No one measure of environmental conditions proved adequate to predict offset and I ultimately developed two separate scenarios which could induce offset and which reasonably predicted the observed dates: 1) hot, dry conditions or 2) cold weather. Scenario 1 is triggered when:

$$(9) \quad \text{PPTSUM}_{\text{prev}} < 1.1 \text{ cm} \ \& \ \text{PPTSUM}_{\text{next}} < 0.5 \text{ cm} \ \& \ \text{TMAX} \geq 0.94 \text{TMAX}_{\text{avg}}$$

where $PPTSUM_{prev}$ is the precipitation total of the previous 31 days, $PPTSUM_{next}$ is the precipitation total of the next seven days, and $TMAX_{avg}$ is the 1990-1992 average highest temperature. Scenario 1 requires low PPT for the previous month, low PPT for the next week, and temperatures approaching annual maximums. Scenario 2 is triggered when:

$$(10) \quad \sum_{i=1}^j TMIN \leq TMIN_{avg} \& Yearday \geq 243$$

where $TMIN$ is daily minimum temperature and $TMIN_{avg}$ is the annual average minimum temperature. A yearday minimum is included to avoid predicting offset in late spring, an event which was not observed at any site. I initially attempted to retain the woodland/pasture sites in the analysis, but this resulted in an MAE of 19.4 days. After removing these two sites, offset MAE dropped dramatically to 7.5 days with an r^2 of 0.89 (Fig. 7d).

CROP: I was unable to develop phenology models capable of predicting the satellite-observed dates of onset and offset. Application of grassland phenology routines provided the best approximation. In the 12 crop sites, grassland routines yielded MAE of 25.3 days for onset and 33.6 days for offset.

DESERT: Modeling results for the desert biome were worse than for crops. Best approximations were produced by modification of grassland equations : in Eq. 8, k was increased to 0.2 and in Eq. 9, $PPTSUM_{prev}$ and

$PPTSUM_{next}$ were reduced to 0.2 cm. With this application, MAE is 26.8 days for onset and 44.8 days for offset.

Continental application of the final biome-level phenology equations reveals extensive interannual variability in vegetation dynamics (Fig. 8). Onset of greenness, though relatively spatially consistent in the East, was earliest in 1990 and latest in 1992. In the West, onset was spatially and temporally variable. Onset in the Big Bend area of Texas, for example, ranged from July in 1990 to May in 1992. In general, onset in the west occurred earlier in 1992 than in 1990 or 1991. One consistent feature, from Montana to Texas, is the inverted green wave, in which onset occurs earliest in the northern great plains, latest around Nebraska, and earlier again to the south. This result was also found by Reed (1994) in a phenological analysis based solely on remote sensing. Offset (Fig. 8) was similarly variable. North - south stratification of offset in the East is a function of photoperiod-induced offset. In both 1990 and 1992 there was extensive interaction of temperature with photoperiod, resulting in an extension of the growing season, especially in the South in 1990 and 1992. Greatest variation, though, again occurred in the West, where variation in precipitation caused significant interannual variation in offset.

Frequency distributions further reveal the extensive interannual variation in growing season length and distribution (Fig. 8). Drought stresses in 1990 led to the prediction that thousands of square kilometers had little or no growing season. The reverse occurred in 1992, when very few pixels had a growing

season less than 50 days. The mean length ranged from 140 days in 1990 to 154 days in 1992. The standard deviation of growing season length followed a trend toward decreasing as growing season length increased: 64 days in 1990, 52 days in 1991, and 42 days in 1992.

Discussion

The purpose of my research was to develop a simple ecosystem phenology model requiring only basic knowledge of landcover, climate, and meteorology. Throughout the research, simplicity and widest possible applicability were predominant concerns. In some cases, maintaining these priorities reduced the absolute accuracy of the model, as when addition of coniferous and mixed forest/cropland increased onset MAE by 0.8 days. Also, by grouping evergreen and deciduous forests, questions of definition are raised. In deciduous canopies, onset and offset are relatively simple: the annual appearance and abscission of leaves. In evergreen landcovers, the picture is not so clear. In western coniferous forests, onset will occur contemporaneously with deciduous understory growth and changes in albedo due to snowmelt (White and Running, 1994; Spanner et al., 1990b) while offset is associated increasing snowcover and understory senescence. In this case, even though the model is predicting seasonality largely unrelated to the spectral response of the dominant vegetation cover, the effective growing season should be accurately captured.

Southern pine forests, on the other hand, do not exhibit strong seasonality in NDVI curves. Ground measurements of Leaf Area Index (LAI) exhibit considerable seasonality (Curran et al., 1992), but if minimum NDVI values are near the NDVI saturation point (described by Huete, 1988; Spanner et al., 1990a; Baret and Guyot, 1991), little or no seasonality will be detected from satellites. Detection of onset or offset with any degree of confidence was not possible with this methodology and southern pine sites were not included in the analysis. Tree equations developed in conifer and deciduous sites are assumed to apply to southern pine stands and should be used to initiate budburst in the spring and cease height growth in the fall. Alternatively, users may choose not to implement seasonality routines in these areas, and rely instead upon internal physiological controls to regulate growth.

Second, the six-class landcover image eliminated the possibility of developing equations for multiple grassland types. As results have suggested, it appears that the grasslands could have been subdivided based on climatic zonation; instead, I used the asymptotic step function to provide a transition between these zones. Inclusion of detailed landcover information, such as that provided by Loveland et al. (1991), might have allowed for more accuracy in model development but would have presented other difficulties. Detailed landcover maps of this type require large amounts of ancillary information that is difficult to acquire over large areas, making regular updates at continental or global scales impractical. More importantly, in many areas of the world, detailed

landcover information is unavailable; basic classification as grassland or forest may be all that is available. The classification presented by Nemani and Running (1995) is purely based on remote sensing; as such, it is globally applicable and annually repeatable.

Figure 7 illustrates that traditional meteorological models can be used to predict satellite observed dates of onset and offset of greenness with an accuracy of about \pm one week in tree and grass biomes. Correlation coefficients are high, except for tree offset, where the range of predicted dates is only 25 days. The exception to traditional modeling is the addition of a radiation summation, which improved MAE by about one day. That short wave radiation summations are similar across tree sites suggests that equal radiation levels translate to a constant greenness, a theory supported by Asrar et al. (1984) who found that increases in NDVI are linearly correlated with increases in absorption of photosynthetically active radiation. Tree models, while based on established techniques from traditional phenology research, are empirically determined and do not necessarily represent the physiological processes which control onset and offset. Commenting on temperature summations, Hunter and Lechowicz (1992) state, "...good predictions can be obtained using the wrong biological model, and in some cases the appropriate causal model may not give good predictions." Photoperiodic controls of offset and interactions with temperature are as poorly understood and as empirically effective as onset temperature summations.

Grassland equations are based on general literature findings with

modifications for satellite phenology detection. Grasslands are often composed of numerous species which occupy different portions of the growing season. Onset obviously occurs when the first species initiate growth, and is relatively simply modeled with a temperature and PPT summation. Growth continues until a hot dry spell is encountered, which will cause wilting point and brownoff of grasses. A further PPT event, though, can cause regrowth of the same or other species. If regrowth occurs, it is likely that the BISE algorithm will treat the brief drop in NDVI as an aberration and the $NDVI_{ratio}$ will not drop below 0.5. For this reason, I included the requirement that the next week, as well as the previous month, must be dry in order to induce offset. In this manner, regrowth is allowed to occur, continuing the main growing season. In some cases, no drought is encountered and the growing season is curtailed by cold weather.

All methodologies for detecting phenological development from satellites are somewhat arbitrary. Simply choosing a methodology and then developing meteorological models to predict those observations would yield little information about exactly what is being predicted. For that reason, I chose to include the field observations from the Harvard Forest and Hubbard Brook. These data, while certainly not a field validation, do suggest that 1) observed onset occurs after initial budburst, during initial leaf expansion and that 2) offset is observed between 15% and 50% leaf fall. Unfortunately, no similar data were available for grassland sites; similar canopy conditions may or may not exist at 0.5 $NDVI_{ratio}$. It is important to note that this methodology predicts the state, not the activity, of

vegetation. Immediately after onset and before offset, the state of the ecosystem may be green, but photosynthetic activity is likely to be dramatically different. In deciduous canopies, with leaf life span less than one year, photosynthetic capacity is highest in newly expanded leaves and much lower in leaves approaching abscission (Reich et al., 1995). Implementation of these phenology equations in ecosystem simulation models should take this into account.

The inability of the methodology to produce phenology routines for desert and crop areas is unsurprising. In desert areas, large amounts of bare soil of varying brightness and accompanying remote sensing difficulties (Huete et al., 1992) interact with low NDVI signals to produce temporal curves which are difficult to accurately interpret. Desert vegetation dynamics are strongly controlled by precipitation, which presents two problems for the methodology. First, desert precipitation is often highly localized and irregular (Barry and Chorley, 1992). The 10km pixel resolution of the study precludes small scale accuracy. Second, prediction accuracy is lowest in areas of low station density, which occur mostly in desert areas. Low station density, combined with low precipitation, inevitably lead to difficulties in predicting *POP*. Errors in precipitation interpolation combined with remote sensing problems lead to problems in model development.

Crops present problems of a different sort. An underlying assumption of the methodology is that the vegetation being modeled is responding to

environmental cues in a deterministic fashion. Crops do not behave this way. Rather, crops are genetically engineered species whose date of onset is controlled by planting dates, fertilization, and irrigation. Offset is not controlled by photoperiod, temperature, or precipitation; harvest dates are the primary factors. Onset and offset, then, are diverged from natural vegetation and cannot realistically be modeled with this methodology. Detailed information about crop type, irrigation, and farming method are required to accurately model crop phenology.

Fortunately, for many of the envisioned user of this methodology, these liabilities should not be a major concern. Large-scale ecosystem simulation models often use potential vegetation maps as their landcover layer and ignore crops entirely. A recent global simulation estimated that only 11% of global net primary production (NPP) was produced in crop and desert biomes (Prince et al., 1995). In their application, use of the modified grassland phenology models should not lead to major errors in NPP estimates. In fact, forest and grass landcover types accounted for 85% of estimated NPP in the study, underscoring the usefulness of developing phenology equations for these biomes. Local applications which must model seasonality for deserts or crops will require detailed crop data including species, planting dates, fertilization, etc. and finer scale precipitation data.

This research was undertaken as an initial test of the methodology. It appears that satisfactory results can be obtained in the continental U.S., but

caution should be exercised before applying these equations beyond the mid-latitude temperate zone in which they were developed. In contrast to mid-latitude forests, for example, photoperiodic controls of offset in the northern boreal forest vary with latitude (Heide, 1974; Hänninen et al., 1990; Oleksyn et al., 1992). In dry tropical areas, phenology is predominantly controlled by highly seasonal precipitation which can result in multiple growing seasons (Reich, 1994). Seasonality in wet tropical forests may be due to poorly understood autogenic physiological controls (Reich, 1994) or optimization of radiation absorption (Wright and van Schaik, 1992). Including these types of dynamics will enable global application of meteorological phenology models.

Summary and Conclusions

Accurate representation of interannual variation in vegetation dynamics is an important parameter in many earth science applications. This research shows that phenology models using traditional applications of daily meteorology and basic climatic variables can reasonably predict satellite-observed onset and offset of greenness in tree and grass biomes with an accuracy of \pm one week. Onset and offset in crop and desert biomes was predicted with an accuracy of only \pm one month. Continental application of the models revealed that 1) onset and offset are spatially and temporally variable and are intimately connected to climate and 2) mean continental growing season length varied by as much as two weeks from 1990-1992. Major assumptions of the methodology are:

- Point and species-level phenology models are scaleable to a regional level
- One average NDVI curve for a 20km x 20km satellite observation site is representative of regional greenness
- A threshold method can be used to assess onset and offset of greenness
- Models developed for a limited number of sites at each landcover are applicable to continental scales
- Subjectivity fitting one asymptotic step function to predict grassland thermal summations adequately captures thermal requirements of different grassland types

Future research should focus on quantifying prediction errors associated with altering onset and offset detection methodologies. Variations in threshold selection and detecting rapid changes in NDVI slope are two areas of planned research. Further testing and development are required before the models are applied outside the mid-latitude proof-of-concept.

References

- Asrar, G., M. Fuchs, E.T. Kanemasu, and J.L. Hatfield. 1984. Estimating absorbed photosynthetic radiation and leaf area index from spectral reflectance in wheat. *Agronomy Journal* 76:300-306.
- Barry, R.G. and R.J. Chorley. 1992. Atmosphere, Weather, and Climate. Routledge, New York. pp. 219-220.
- Bristow, K.L. and G.S. Campbell. 1984. On the relationship between incoming solar radiation and daily maximum and minimum temperature. *Agricultural and forest meteorology* 31:159-166.
- Brown, D.M. 1986. Corn yield responses to irrigation, plant population and nitrogen in a cool, humid climate. *Canadian Journal of Plant Science* 66:453-464.
- Burk, J.H. 1982. Phenology, germination, and survival of desert ephemerals in deep canyon, riverside county, California. *Madrono* 29:154-163.
- Cannel, M.J.R. and R.I. Smith. 1986. Climatic warming, spring budburst and frost damage on trees. *Journal of Applied Ecology* 23:177-191.
- Caprio, J.M. 1993. Flowering dates, potential evapotranspiration and water use efficiency of *Syringa vulgaris* L. at different elevations in the western United States of America. *Agricultural and Forest Meteorology* 63:55-71.
- Curran, P.J., J.L. Dungan, and H.L. Gholz. 1992. Seasonal LAI in Slash Pine estimated with Landsat TM. *Remote Sensing of Environment* 39:3-13.
- Dickinson, C.E. and J.L. Dodd. 1976. Phenological patterns in the shortgrass prairie. *American Midland Naturalist* 96:367-378.
- Doraiswamy, P.C. and D.R. Thompson. 1982. A crop moisture stress index for large areas and its application in the prediction of spring wheat phenology. *Agricultural Meteorology* 27:1-15.
- Duncan, J., D. Stow, J. Franklin, and A. Hope. 1993. Assessing the relationship between spectral vegetation indices and shrub cover in the Jornada Basin, New Mexico. *International Journal of Remote Sensing* 14:3395-3416.
- Fischer, A. 1994. A model for the seasonal variations of vegetation indices in coarse resolution data and its inversion to extract crop parameters. *Remote Sensing of Environment* 48:220-230.

- French, N. and R.H. Sauer. 1974. Phenological studies and modeling in grasslands. In Phenology and Seasonality Modeling. H. Leith, ed. Springer-Verlag, New York. pp. 227-236.
- Glassy, J.M. and S.W. Running. 1994. Validating diurnal climatology logic of the MT-CLIM model across a climatic gradient in Oregon. *Ecological Applications* 4(2):248-257.
- Goetz, S.J. and S.D. Prince. 1996. Remote sensing of net primary production in boreal forest stands. *Agricultural and Forest Meteorology* 78:149-179.
- Goward, S.N., C.J. Tucker, D.G. Dye. 1985. North American vegetation patterns observed with the NOAA advanced very high resolution radiometer. *Vegetation* 64:3-14.
- Goward, S.N., B. Markham, D.G. Dye, W. Dulaney, and J. Yang. 1991. Normalized difference vegetation index measurements from the Advanced Very High Resolution Radiometer. *Remote Sensing of Environment* 35:257-277.
- Baret, F. and G. Guyot. 1991. Potentials and limits of vegetation indices for LAI and APAR assessment. *Remote Sensing of Environment* 35:161-173.
- Hänninen, H., R. Häkkinen, P. Hari, and V. Koski. 1990. Timing of growth cessation in relation to climatic adaptation of northern woody plants. *Tree Physiology* 6:29-39.
- Hänninen, H., S. Kellomäki, K. Laitinen, B. Pajari, and T. Repo. 1993. Effect of increased winter temperature on the onset of height growth of Scots pine: a field test of a phenological model. *Silva Fennica* 27:251-257.
- Hari, P. and R. Häkkinen. 1991. The utilization of old phenological time series of budburst to compare models describing annual cycles of plants. *Tree Physiology* 8:281-287.
- Heide, O.M. 1974. Growth and dormancy in Norway Spruce ecotypes (*Picea abies*) I. Interaction of photoperiod and temperature. *Physiologia Plantarum* 30:1-12.
- Henderson-Sellers, A. Z.-L. Yang, and R.E. Dickinson. 1993. The project for intercomparison of land-surface parameterization schemes. *Bulletin of the American Meteorological Society* 74:1335,1349.

- Hicken, R.P. and M.T. Vittum. 1976. The importance of soil and air temperature in spring phenoclimatic modeling. *International Journal of Biometeorology* 20:200-206.
- Hodges, T. and V. French. 1985. Soyphen: soybean growth stages modeled from temperature, daylength, and water availability. *Agronomy Journal* 77:500-505.
- Holben, B.N. 1986. Characteristics of maximum-value composite images from temporal AVHRR data. *International Journal of Remote Sensing* 7:1417-1434.
- Hood, J.J. 1993. Advanced very high resolution radiometer validation data set. 25th International Symposium, Remote Sensing and Global Environmental Change. Graz, Austria: 4-8 April.
- Huete, A.R. 1988. A soil-adjusted vegetation index (SAVI). *Remote Sensing of Environment* 25:295-309.
- Huete, A.R., G. Hua, J. Qi, A. Chehbouni, and W.J.D.G. Van Leeuwem. 1992. Normalization of multidirectional red and NIR reflectances with the SAVI. *Remote Sensing of Environment* 40:1-20.
- Hungerford, R.D., R.R. Nemani, S.W. Running, and J.C. Coughlan. 1989. MTCLIM: a mountain microclimate simulation model. USDA Forest Service Research Paper INT-414. Intermountain Forest and Range Experiment Station. U.S. Department of Agriculture, Forest Service, Ogden Utah.
- Hunter, A.H. and M.J. Lechowicz. 1992. Predicting the timing of budburst in temperate trees. *Journal of Applied Ecology* 29:597-604.
- Justice, C.O., J.R.G. Townshend, B.N. Holben, and C.J. Tucker. 1985. Analysis of the phenology of global vegetation using meteorological satellite data. *International Journal of Remote Sensing* 6:1271-1318.
- Kaduk, J. and M. Heimann. 1996. A prognostic phenology model for global terrestrial carbon cycle models. *Climate Research* 6:1-19.
- Kemp, P.R. 1983. Phenological patterns of Chihuahuan desert plants in relationship to the timing of water availability. *Journal of Ecology* 71:427-436.
- Koski, V. and J. Selkänaho. 1982. Experiments on the joint effect of heat sum and photoperiod on seedlings of *Betula pendula*. *Communications Instituti Forestalis Fenniae*. 105:1-34.

- Lavender, D.P. 1981. Environment and shoot growth of woody plants. Research Paper 45, Forest Research Lab, School of Forestry. Oregon State University.
- Lindsay, A.A. and J.E. Newman. 1956. Uses of official weather data in spring time - temperature analysis of an Indiana phenological record. *Ecology* 37:812-823.
- Lloyd, D. 1990. A phenological classification of terrestrial vegetation cover using shortwave vegetation index imagery. *International Journal of Remote Sensing* 11:2269-2279.
- Lomas, J. and H. Herrera. 1985. Weather and rice yield relationships in tropical Costa Rica. *Agricultural and Forest Meteorology* 35:133-151.
- Loveland, T.R., J.W. Merchant, D.O. Ohlen, and J.F. Brown. 1991. Development of a land-cover characteristics database for the conterminous U.S. *Photogrammetric Engineering & Remote Sensing* 57:1453-1463.
- Markon, C.J., M.D. Fleming, and E.F. Binnian. 1995. Characteristics of vegetation phenology over the Alaskan landscape using AVHRR time-series data. *Polar Record* 31:179-190.
- Mueggler, W.F. 1983. Variation in production and seasonal development of mountain grasslands in western Montana. USDA Forest Service Research Paper INT-316. Intermountain Forest and Range Experiment Station. U.S. Department of Agriculture, Forest Service, Ogden Utah.
- Murray, M.B., M.J.R. Cannel, and R.I. Smith. 1989. Date of budburst of fifteen tree species in Britain following climatic warming. *Journal of Applied Ecology* 26:693-700.
- Myneni, R.B. and D.L. Williams. 1994. On the relationship of FAPAR and NDVI. *Remote Sensing of Environment* 49:200-211.
- Nemani, R.R. and S.W. Running. 1995. Satellite monitoring of global land cover changes and their impact on climate. *Climate Change* 31:395-413.
- Nooden, L.D. and J.A. Weber. 1978. Environmental and hormonal control of dormancy release in terminal buds of plants. *Dormancy and Development Arrest*. M.E. Clutter (ed.). Academic Press, New York, New York.

- O'Leary, G.J., D.J. Connor, and D.H. White. 1985. Effect of sowing time on growth, yield and water use of rain-fed wheat in the Wimmera, Vic. *Australian Journal of Agricultural Research* 36:187-196.
- Oleksyn, J., M.G. Tjoelker, and P.B. Reich. 1992. Growth and biomass partitioning of populations of European *Pinus sylvestris* L. Under simulated 50° and 60° N daylengths: evidence for photoperiodic ecotypes. *New Phytologist* 120:561-574.
- Prince, S.D., S.j. Goetz, and S.N. Goward. 1995. Monitoring primary productivity from earth observing satellites. *Water, Air, and Soil Pollution* 82:509-522.
- Ram, J., S.P. Singh, and J.S. Singh. 1988. Community level phenology of grassland above treeline in central Himalaya, India. *Arctic Alpine Research* 20:325-332.
- Reaumur, M. 1735. Observations du thermometre, faites a Paris pendant l'annee 1735. *Mem Acad. Royal Science Paris* 737-754.
- Reed, B.C., J.F. Brown, D. VanderZee, T.R. Loveland, J.W. Merchant, and D.O. Ohlen. 1994. Measured phenological variability from satellite imagery. *Journal of Vegetation Science* 5:703-714.
- Reich, P.B. 1994. Phenology of tropical forests: patterns, causes, and consequences. *Canadian Journal of Botany* 73:164-174.
- Reich, P.B., T. Koike, S.T. Gower, and A.W. Schoettle. 1995. Causes and consequences of variation in conifer leaf life-span. In Ecophysiology of Coniferous Forests. W.K. Smith and T.M. Hinckley, eds. Academic Press, New York. pp. 225-254.
- Running, S.W., Nemani, R.R. and Hungerford, R.D. 1987. Extrapolation of synoptic meteorological data in mountainous terrain and its use for simulating forest evapotranspiration and photosynthesis. *Canadian Journal of Forest Research*, 17:472-483.
- Running, S.W., and R.R. Nemani. 1991. Regional hydrologic and carbon balance responses of forests resulting from potential climate change. *Climatic Change* 19:349-368.

- Schmidt, W.C. and J.E. Lotan. 1980. Phenology of common forest flora of the Northern Rockies -- 1928 to 1937. USDA Forest Service Research Paper INT-259. Intermountain Forest and Range Experiment Station. U.S. Department of Agriculture, Forest Service, Ogden Utah
- Schwartz, M.D. 1992. Phenology and springtime surface-layer change. *Monthly Weather Review* 120:2570-2578.
- Sellers. P.J., L. Bounoua, G.J. Collatz, D.A. Randall, D.A. Dazlich, S.O. Los, J.A. Berry, I. Fung, C.J. Tucker, C.B. Field, and T.G. Jensen. 1996. Comparison of radiative and physiological effects of doubled atmospheric CO₂ on climate. *Science* 271:1402-1406.
- Sharifi, M.R., F.C. Meinzer, E.T. Nilsen, P.W. Rundel, R.A. Virginia, W.M. Jarrell, D.J. Herman, and P.C. Clark. 1988. Effect of manipulation of water and nitrogen supplies on the quantitative phenology of *Larrea tridentata* (creosote bush) in the Sonoran Desert of California. *American Journal of Botany* 75:1163-1174.
- Sims, P.L. 1988. Grasslands. In North American Terrestrial Vegetation. M.G. Barbour and W.D. Billings eds. Cambridge University Press, Cambridge. pp. 265-286
- Smit-Spinks, B., B.T. Swanson, and A.H. Markhart III. 1985. The effect of photoperiod and thermoperiod on cold acclimation and growth of *Pinus sylvestris*. *Canadian Journal of Forest Research* 15:453-460.
- Spanner, M.A., L.L. Pierce, D.L. Peterson, and S.W. Running. 1990a. Remote sensing of temperate coniferous forests: the influence of canopy closure, understory vegetation and background reflectance. *International Journal of Remote Sensing* 11:95-111.
- Spanner, M.A., L.L. Pierce, S.W. Running, and D.L. Peterson. 1990b. The seasonality of AVHRR data of temperate coniferous forests: relationships with leaf area index. *Remote Sensing of Environment* 33:97-112.
- Sparks, T.H. and P.D. Carey. 1995. The response of species to climate over two centuries: an analysis of the Marsham phenological records, 1736-1947. *Journal of Ecology* 83:321-329.
- Stone, T.A., S. Schlesinger, R.A. Houghton, and G.M. Woodwell. 1994. A map of the vegetation of South America based on satellite imagery. *Photogrammetric Engineering & Remote Sensing* 60:541-551.

- Thomson, A.J. and S.M. Moncrieff. 1981. Prediction of budburst in Douglas-fir by degree-day accumulation. *Canadian Journal of Forest Research* 12:448-452.
- Thornton, P.E., S.W. Running, and M.A. White. 1995. Generating surfaces of daily meteorological variables over large regions of complex terrain. *Journal of Hydrology*. In press.
- Tucker, C.J., J.R.G. Townshend, and T.E. Goff, 1985. African land-cover classification using satellite data. *Science* 227: 369-375,
- Undersander, D.J. and S. Christiansen. 1986. Interactions of water variables and growing degree days on heading phase of winter wheat. *Agricultural and Forest Meteorology* 38:169-180.
- Valentine, H.T. 1983. Budbreak and leaf growth functions for modeling herbivory in some gypsy moth hosts. *Forest Science* 29:607-617.
- Vegis, A. 1964. Dormancy in Higher Plants. *Annual Review of Plant Physiology* 15:185-222.
- VEMAP Modeling Participants. 1995. Vegetation/ecosystem modeling and analysis project: Comparing biogeography and biogeochemistry models in a continental-scale study of terrestrial ecosystem responses to climate change and CO₂ doubling. *Global Biogeochemical Cycles* 9:407-437.
- Viouy, N. and O. Arino. 1992. The best index slope extraction (BISE): a method for reducing noise in NDVI time-series. *International Journal of Remote Sensing* 13:1585-1590.
- White, J.D. and S.W. Running. 1994. Testing scale dependent assumptions in regional ecosystem simulation models. *Journal of Vegetation Science* 5:687-702.
- Wright, S.J. and C.P. van Schaik. 1992. Light and the phenology of tropical trees. *The American Naturalist* 143:192-199.
- Yoder, B.J. and R.H. Waring. 1994. The normalized difference vegetation index of small Douglas-Fir canopies with varying chlorophyll concentrations. *Remote Sensing of Environment* 49:81-91.

Zheng, D., E.R. Hunt, and S.W. Running. 1993. A daily soil temperature model based on air temperature and precipitation for continental applications. *Climate Research* 2:183-191.

Table 1: Satellite phenology detection methodologies

METHOD	REFERENCE
0.17 NDVI threshold	Fischer, 1994
0.09 NDVI threshold	Markon et al., 1995
0.099 NDVI threshold	Lloyd, 1990
divergence of smoothed curve from autoregressive moving average	Reed et al., 1994
largest NDVI increase after air temperature exceeds 5°C	Kaduk and Heimann, 1996

Table 2: Hubbard Brook Experimental Forest
phenology measurement scheme

Spring Phenological Stages	
0	unexpanded buds
1	bud swelling noticeable
2	small leaves or flowers visible, leaves about 1cm long
3	leaves half of final length, about 5 cm long, and obscure half of sky through canopy
4	summer canopy conditions, full leaf expansion, little sky visible through canopy
Fall Phenological Stages	
4	summer canopy conditions, scattered color changes
3	many leaves colored, much green still present
2	most leaves colored, few fallen, most of sky still obscured through canopy
1	no green present in leaves, half fallen, half of sky visible through canopy
0.5	most leaves fallen
0	all leaves except remnants fallen, winter conditions

Table 3: MT-CLIM 3d cross validation results

	Daily predictions from daily observation		Annual predictions from daily observations		Annual predictions from annual observations	
	MAE	BIAS	MAE	BIAS	MAE	BIAS
1990						
TMAX (°C)	1.93	1.3×10^{-5}	0.78	0.0047	0.78	0.0047
TMIN (°C)	1.81	-8.5×10^{-6}	1.00	-0.0031	1.00	-0.0031
PPT (%)	NA	NA	21.3	4.0	21.8	9.9
PPT (cm)	NA	NA	13.1	-2.5	12.5	-0.14
1991						
TMAX (°C)	1.91	1.7×10^{-5}	0.77	0.0063	0.77	0.0063
TMIN (°C)	1.76	-1.3×10^{-5}	0.97	-0.0049	0.97	-0.0049
PPT (%)	NA	NA	18.4	1.1	18.8	6.2
PPT (cm)	NA	NA	13.5	-3.3	13.0	-0.66
1992						
TMAX (°C)	1.88	-1.4×10^{-5}	0.77	-0.0052	0.77	-0.0052
TMIN (°C)	1.76	-3.3×10^{-5}	0.99	-0.012	0.99	-0.012
PPT (%)	NA	NA	18.5	3.0	19.0	7.2
PPT (cm)	NA	NA	12.9	-1.8	12.5	0.1

Best Index Slope Extraction from raw AVHRR data

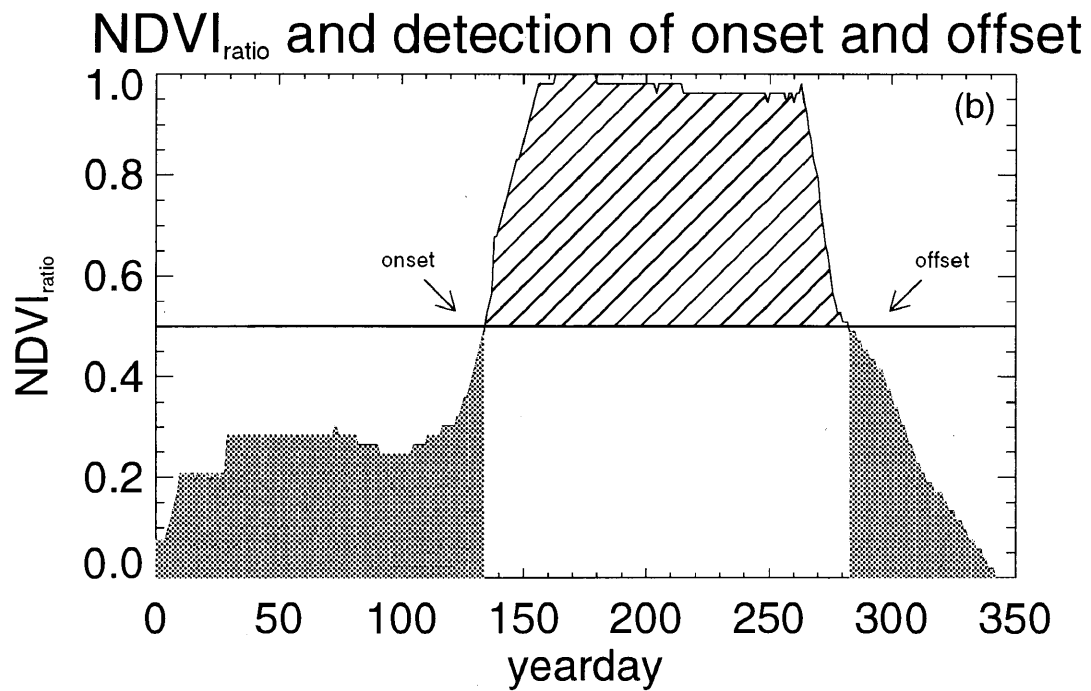
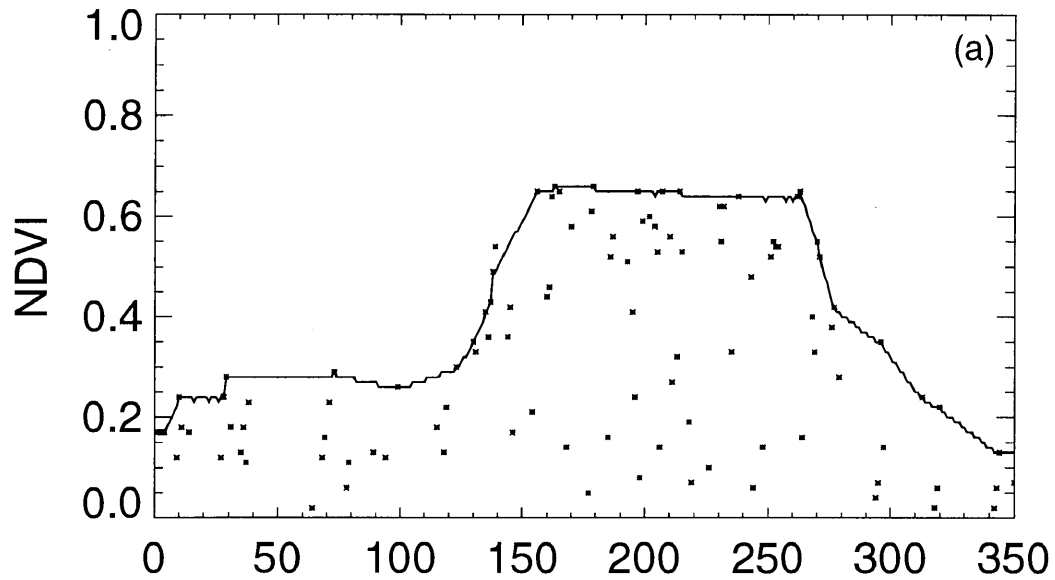


Fig. 1

Weather Station Distribution

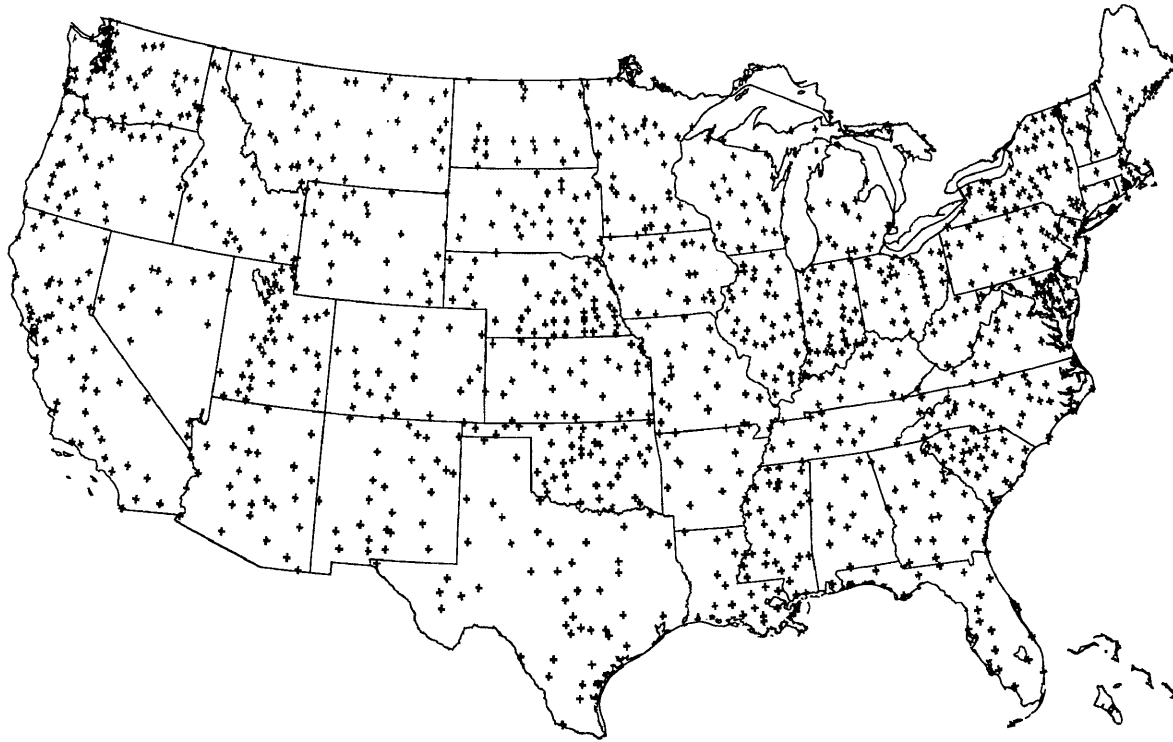
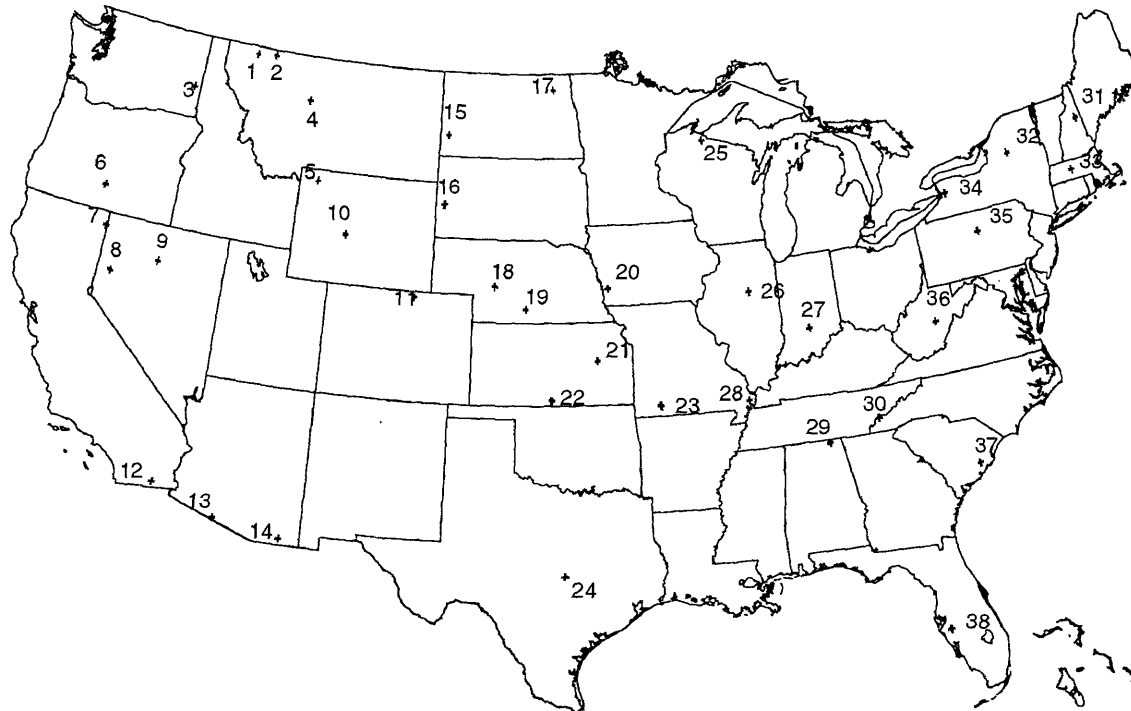


Fig. 2

Satellite Phenology Observation Sites



TREE BIOME

Western Conifer (1,16)
 Conifer Forest (5)
 Northern Forest (25)
 Northern Hardwood (31,32)
 Mixed Hardwood (27,29,30,36)
 Deciduous Forest (33)
 Mixed Forest/Cropland (23)

CROP BIOME

Crop (12,17,18,20,21,22,28,34)
 Crop/Pasture (3)
 Crop/Woodland (24,37,38)

GRASS BIOME

Grass (2,4,11,15,19)
 Woodland/Pasture (26,35)

DESERT BIOME

Desert shrubs/grass (6,7,8,9,10,14)
 Desert shrubs (13)

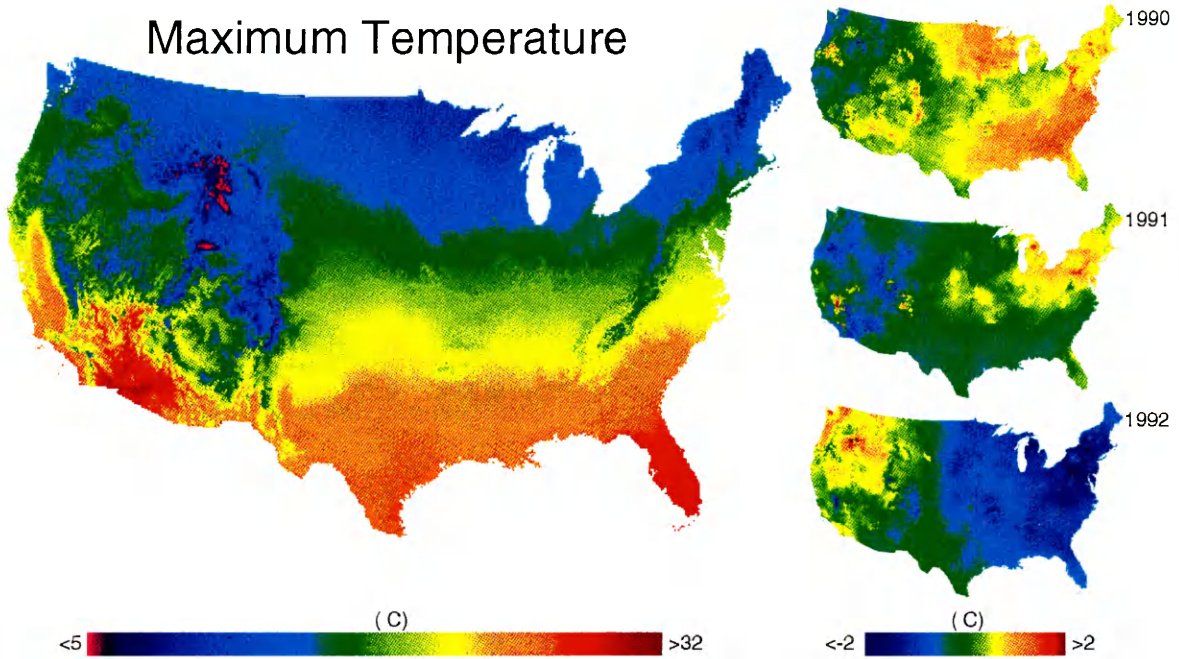
landcover from Hood, 1993

Fig.3

THREE-YEAR MEAN (1990-1992)

DIFFERENCE FROM MEAN

Maximum Temperature



Precipitation

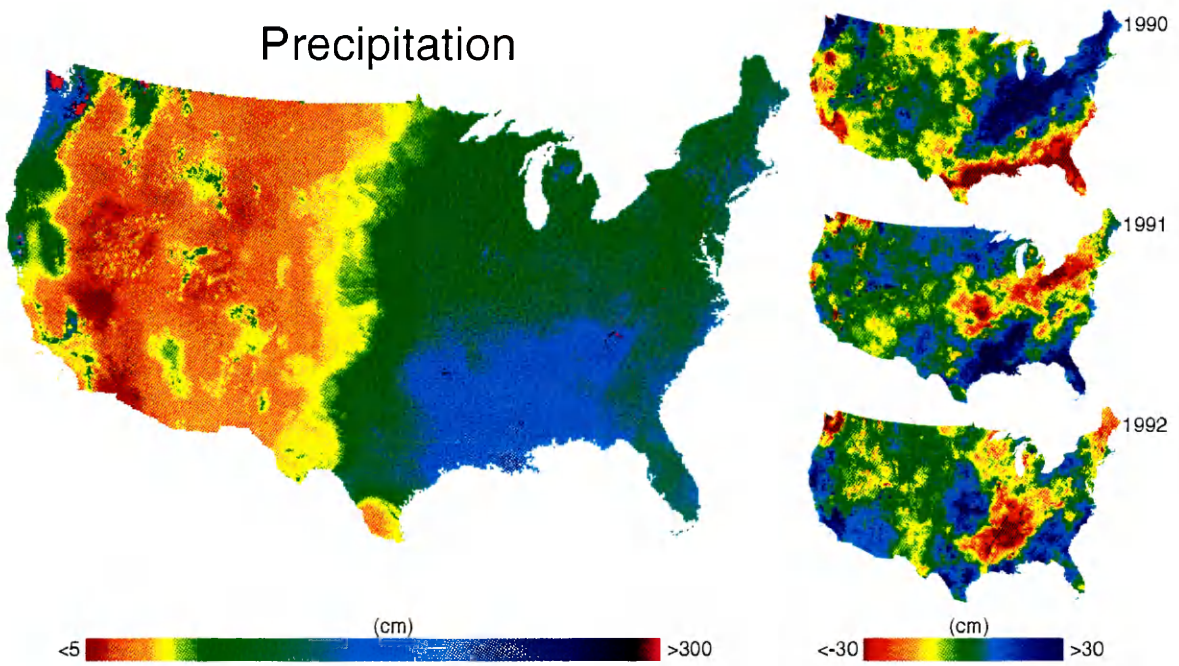
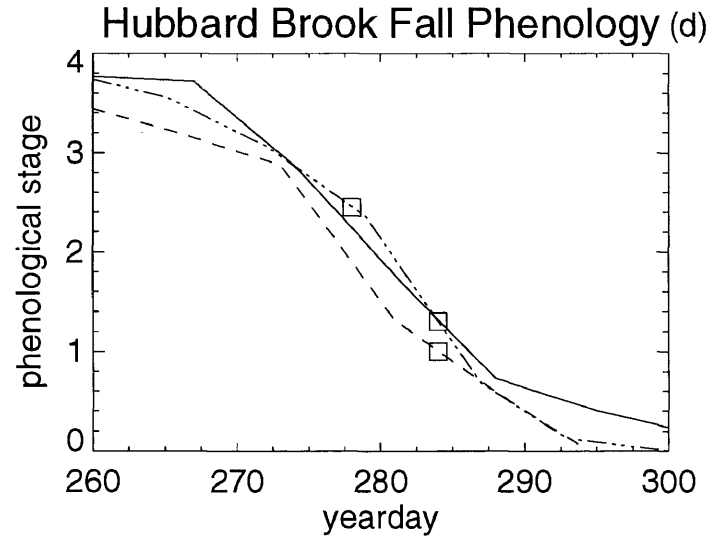
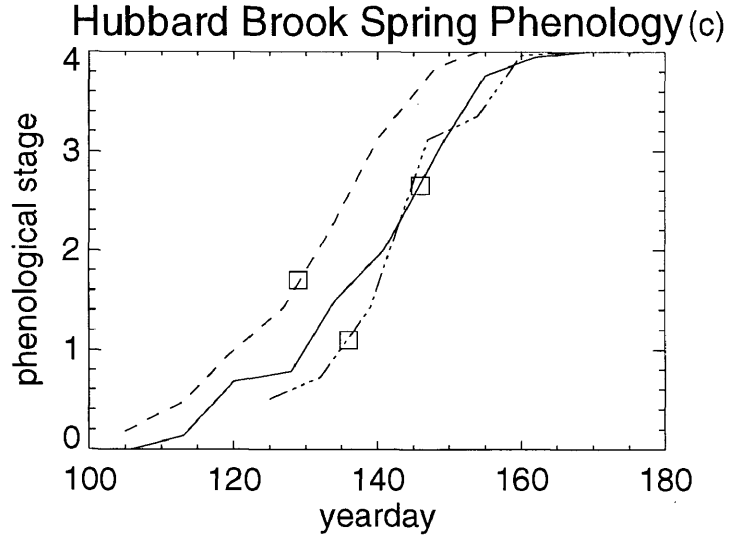
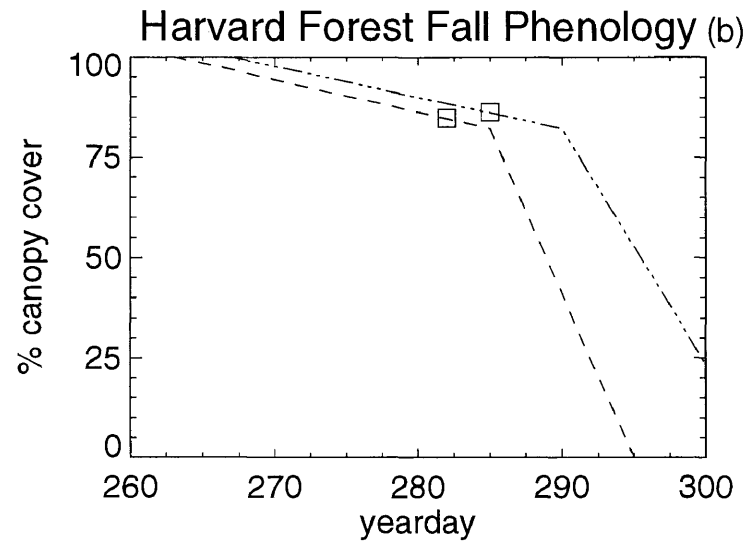
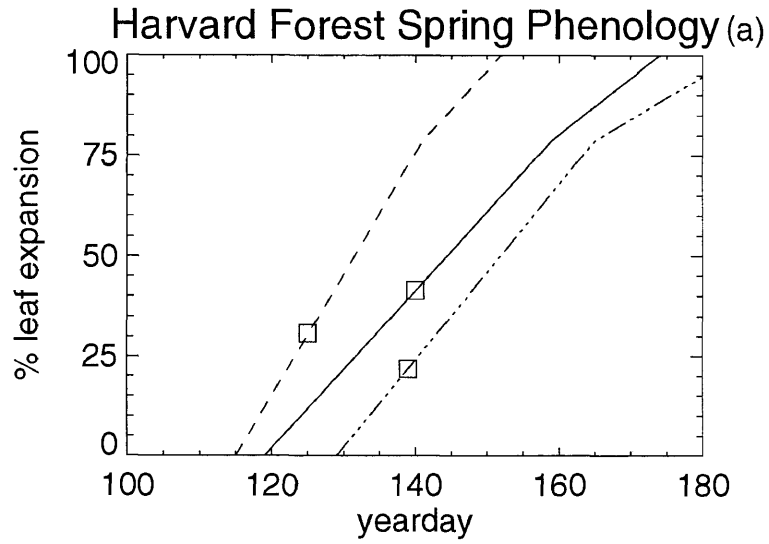


Fig. 4



1990 ——— 1991 - - - - 1992 - · - - -

Fig. 5

TAVG (1990–1992) vs. Soil Temp Summation at Onset

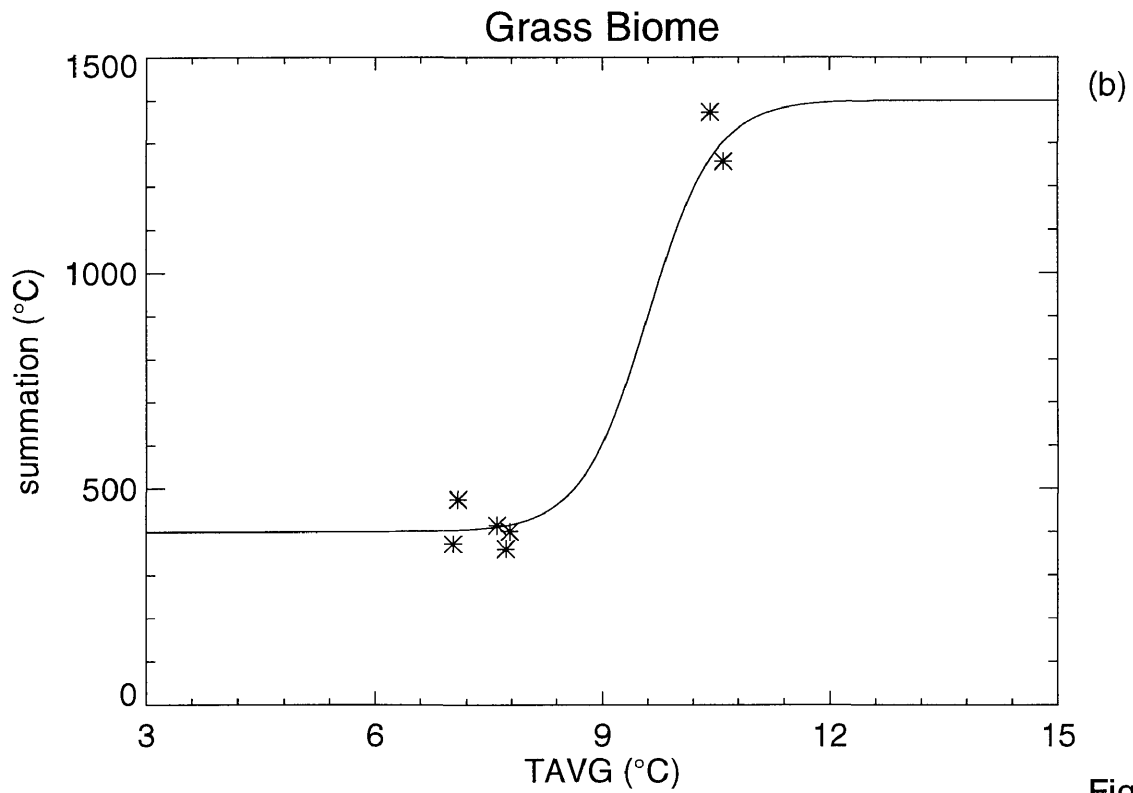
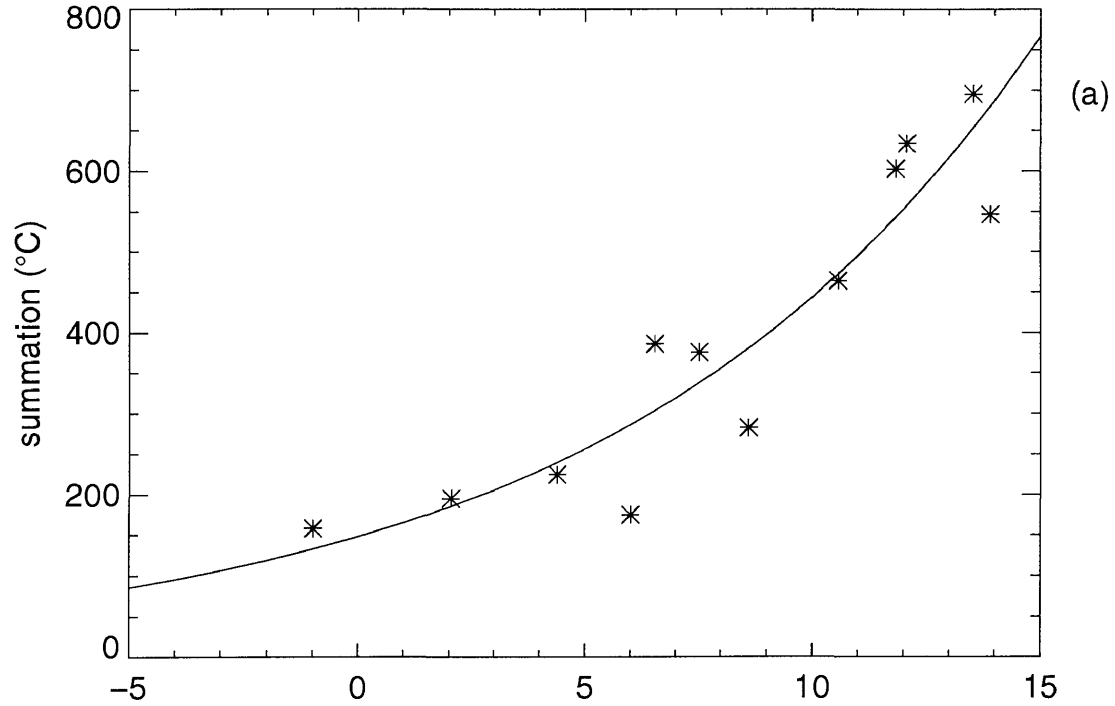


Fig. 6

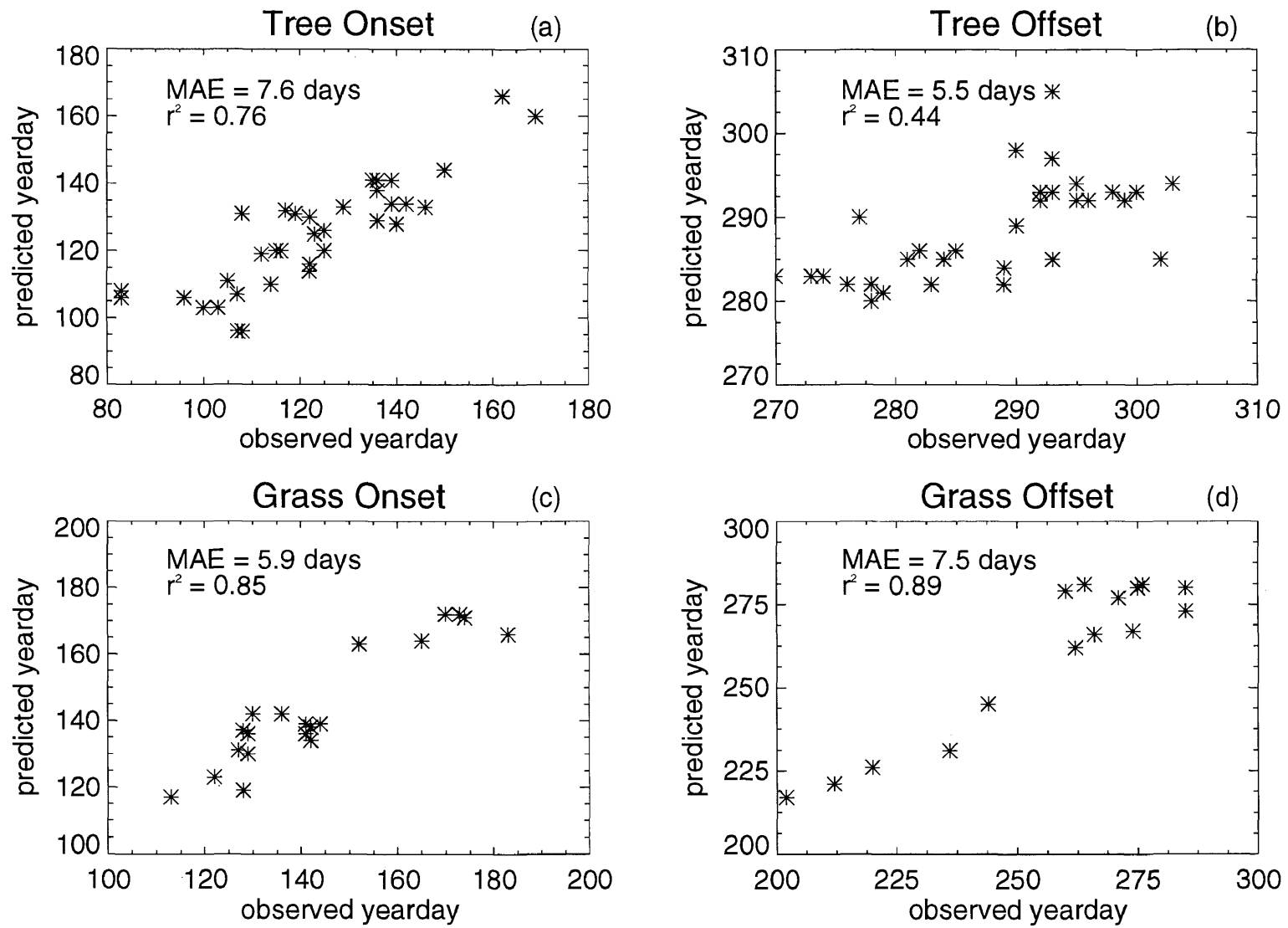


Fig. 7

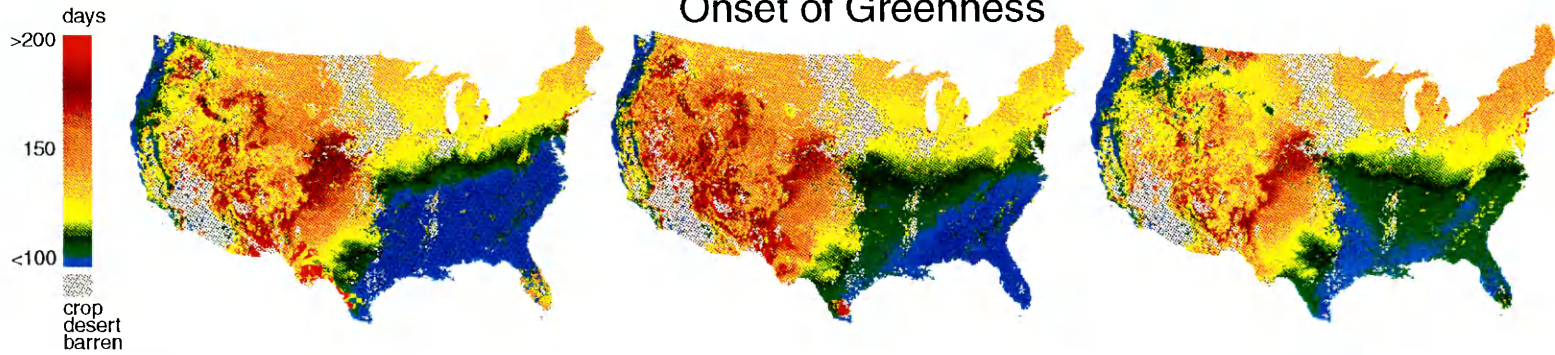
CONTINENTAL PHENOLOGY

1990

1991

1992

52



Growing Season Frequency Distribution

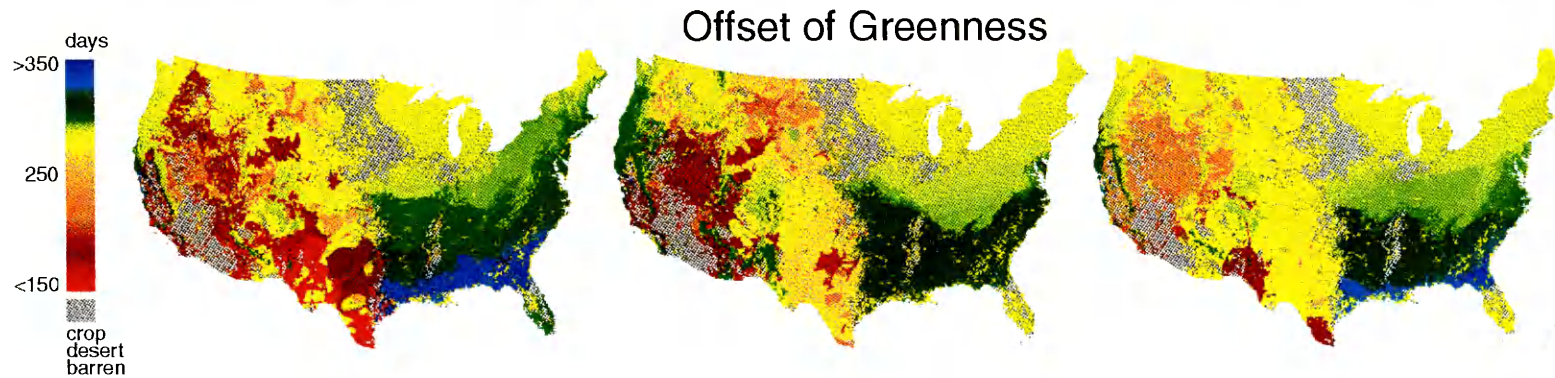
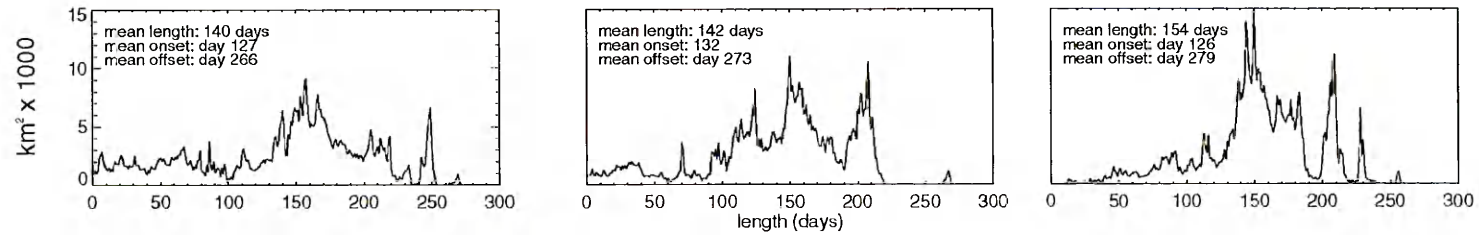


Fig. 8